



ELSEVIER

International Journal of Pharmaceutics 175 (1998) 255–267

**international
journal of
pharmaceutics**

Difference in the transport of metal and free-base porphyrins Steady-state and time-resolved fluorescence studies

Irén Bárdos-Nagy, Rita Galántai, András D. Kaposi, Judit Fidy *

Institute of Biophysics, Semmelweis Medical University, P.O. Box 263, Budapest H-1444, Hungary

Received 15 April 1998; received in revised form 2 September 1998; accepted 2 September 1998

Abstract

The binding of Mg-mesoporphyrin and mesoporphyrin to the primary binding site of human serum albumin (HSA) has been studied in the absence and in the presence of 1,2-dimyristoyl-sn-glycero-3-phosphatidylcholine/1,2-dimyristoyl-sn-glycero-3-phosphatidylglycerol (DMPC/DMPG) liposomes. The equilibrium constants of Mg-mesoporphyrin IX (MgMP) and mesoporphyrin IX (MP) for association to HSA were $1.7 \cdot 10^7$ (M^{-1}) and $2.5 \cdot 10^7$ (M^{-1}), respectively. The association constants for binding to the liposomes were: $1.5 \cdot 10^4$ (M^{-1}) for MgMP, and $3.2 \cdot 10^4$ (M^{-1}) for MP. The smaller value for the association constants of the MgMP relative to MP in both processes are interpreted as the effect of an out of plane position of Mg^{2+} and possible ligand co-ordination. HSA added to the liposomes with incorporated porphyrins results in the redistribution of bound molecules. For the MgMP this distribution can be interpreted by the competition of two independent binding processes, while the binding kinetics of MP significantly deviates from this model. The difference is explained by supposing a specific interaction between HSA and the liposomes in case of the free-base MP. © 1998 Elsevier Science B.V. All rights reserved.

Keywords: Fluorescence; Human serum albumin; Liposomes; Mesoporphyrin; Mg-mesoporphyrin

Abbreviations: ALA, 5-aminolaevulinic acid; DMF, dimethyl-formamide; DMPC, 1,2-dimyristoyl-sn-glycero-3-phosphatidylcholine; DMPG, 1,2-dimyristoyl-sn-glycero-3-phosphatidylglycerol; HRP, horseradish peroxidase; HSA, human serum albumin; MgMP, Mg-mesoporphyrin IX; MP, mesoporphyrin IX; PDT, photodynamic therapy; PP, protoporphyrin IX; SUV, small unilamellar vesicles.

* Corresponding author. Tel.: +36 1 2676261; fax: +36 1 2666656; e-mail: judit@puskin.sote.hu

1. Introduction

Both the endogenous synthesis and degradation; both the transport and the binding of porphyrin derivatives have been examined by a vast number of studies for the last few decades because of the widespread biological significance of these processes from photosynthetic systems to human

metabolism (Muller-Eberhard and Morgan, 1975; Ricchelli et al., 1990; Kennedy and Pottier, 1992; Rosenberger and Margalit, 1993; Vever-Bizet and Brault, 1993).

The aspects of the biomedical applications of porphyrin derivatives (e.g. photodynamic therapy, PDT) turned the attention to a broader class of molecules that involved metallo-porphyrins, phthalocyanins and chlorin derivatives of photodynamic activity (Spikes, 1986; Bonett et al., 1989; Kessel et al., 1991; Henderson and Dougherty, 1992; Moan and Berg, 1992; Senge, 1992).

Recently, a new approach was suggested to PDT: the selective induction of natural porphyrin derivatives by the precursor 5-aminolaevulinic acid (ALA) in tumour cells (Fukuda et al., 1992; Kennedy and Pottier, 1992; Loh et al., 1993). Thus the understanding of the metabolism and molecular interactions of endogenous porphyrin species, especially those of photodynamic activity (e.g. protoporphyrin-IX, PP), became equally important with respect to biomedical applications.

It was found that in the selective localisation of the porphyrin derivatives, the lipid compartments of the plasma membranes or of mitochondrial membranes play important role (Moan and Christensen, 1981; Brault, 1990; Geze et al., 1993; Ricchelli, 1995; Rosenbach-Belkin et al., 1996). Due to the complexity of the native biological systems, it is accepted to apply simplified systems as models, that allow to study certain important aspects of these complex phenomena in details.

In this work the partition of free-base mesoporphyrin IX (MP) and a metallo-porphyrin (Mg-mesoporphyrin (MgMP)) photosensitiser has been studied between the lipid phase and human serum albumin (HSA). The role of a metal co-ordination in the transport of porphyrin derivatives is an important point in itself (Reddi et al., 1981; Vever-Bizet and Brault, 1993; Greenbaum and Kappas, 1994a), and recent works suggesting the use of bacteriochlorophyll derivatives in PDT (Rosenbach-Belkin et al., 1996) make the problem of Mg ion co-ordination especially interesting. HSA is a prominent serum protein in metabolic processes and it may also compete with the desired cellular accumulation of the photosensitisers in case of PDT (Muller-Eberhard and Mor-

gan, 1975; Kuzelova and Brault, 1994). In the experiments we used negatively charged 1,2-dimyristoyl-sn-glycero-3-phosphatidylcholine/1,2-dimyristoyl-sn-glycero-3-phosphatidylglycerol (DMPC/DMPG) liposomes, to mimic the properties of mitochondrial membrane (Kagawa, 1974).

It is known that in the case of PP, the native candidate for ALA-induced PDT, both the aggregation and the photoinstability of the molecule impose serious difficulties in the experiments (Rotenberg et al., 1987). We found that for MP monomeric conditions can be achieved in aqueous solution within a concentration range that is appropriate for reliable optical spectroscopic studies and the data are not affected by the photolability of the chromophore. MP is of molecular symmetry similar to that of PP, and there is only a slight difference in hydrophobicity. We believe that it is an acceptable approximation that from the results of these measurements we can also draw conclusions for the behaviour of PP.

2. Materials and methods

2.1. Chemicals

The samples were prepared in 10 mM sodium phosphate buffer at pH 7.4. DMPG, DMPC, 1 × crystallised and lyophilised HSA and MP dihydrochloride were purchased from Sigma (St. Louis, MO), MgMP (disodium salt) was from Porphyrin Products (Logan, UT). All the solvents (chloroform, methanol, ethanol, dimethyl-formamide (DMF)) were obtained from Merck. The chemical components in the samples were of spectroscopic purity. Sephadex G100 Superfine, used to purify HSA, was purchased from Pharmacia Fine Chemicals AB.

2.2. Preparation of porphyrin solutions

Stock solutions of MP were prepared in DMF and that of MgMP in ethanol (for better solubility) and both were kept in dark to avoid photodegradation. For the measurements, the solutions were obtained by dilution with a phosphate buffer

of pH 7.4, and used immediately after preparation. The correct concentration of aqueous porphyrin solutions was determined by using the Soret band absorbance of the dyes in organic solvents. The molar extinction coefficients for MP dissolved in DMF, as $\epsilon_{399} = 1.55 \cdot 10^5 \text{ M}^{-1}\text{cm}^{-1}$, and for MgMP in ethanol as $\epsilon_{407} = 3.02 \cdot 10^5 \text{ M}^{-1}\text{cm}^{-1}$ were determined by us, and used further on for calculations.

The fluorescence intensity was measured in function of the porphyrin concentration and a linear dependence was found below 80 nM for both dyes. This proved the monomeric condition of both porphyrins in this concentration range in accordance with literature data for MP and deuteroporphyrin in aqueous solution at pH 7.2 (Margalit and Rotenberg, 1984). In the measurements we kept the concentration of porphyrin solutions constant at 50 nM, to assure that we had been studying the interactions of MP and MgMP monomers with HSA and liposomes.

2.3. Preparation of HSA solution

HSA has been purified by gel filtration (Sephadex G100 column equilibrated with 10 mM phosphate buffer at pH 7.4), and by SDS gel electrophoresis. The purified fraction was lyophilised and stored at -20°C . The concentration of HSA solutions was determined spectrophotometrically (Reddi et al., 1981).

2.4. Preparation of liposomes

Stock solutions of DMPC/DMPG (19:1) in chloroform/methanol (9:1) were dried to a film using a stream of nitrogen. Lipids were hydrated with buffer by hand-shaking followed by sonication (MSE Desintegrator P. 6/527) until no further decrease of turbidity could be detected. The samples were centrifuged (Beckman J2-21 centrifuge, 19000 rpm, 45 min) to eliminate the remnants of the multi-lamellar vesicles, and Ti particles from the sonicator. The size of the liposomes was determined by light scattering measurements and the average diameter was about 40–50 nm (small unilamellar vesicles (SUV)). By keeping the liposome size at this

small diameter range, the light scattering background was reduced to negligible in the optical spectroscopic measurements. The phospholipid content of liposome suspensions was quantified according to Rouser (Rouser, 1969). For calculations and graphic representations, the molar lipid concentration was used instead of the liposome concentration in all cases when liposomes were used.

2.5. Equipment

Absorption spectra were recorded by a Cary 4E UV-visible spectrophotometer. Fluorescence emission and excitation spectra, kinetic, and lifetime measurements were performed by using an Edinburgh Analytical Instruments (Edinburgh, UK) CD900 luminometer equipped with Xe 75 W light source for steady state measurements and an nF900 40 kHz ns flashlamp for time resolved studies. Correction for inner filter effects has been performed by the formula:

$$I_{\text{corr}} = I_{\text{obs}} \cdot 10^{(A_{\text{ex}} + A_{\text{em}})/2} \quad (1)$$

when the absorbance was above 0.05. I_{corr} and I_{obs} are the corrected and the observed fluorescence intensities, A_{ex} and A_{em} are the absorbances at the excitation and the emission wavelength (Lakowitz, 1983a). The observed fluorescence intensities were corrected also for dilution.

Fluorescence decay curves have been determined by the time correlated single photon counting technique, and the lifetimes were analysed by an FL900CDA software package (Edinburgh Analytical Instruments) using a deconvolution technique. The full width of half maximum (FWHM) value of the lamp function was normally around 1.5 ns.

The temperature of the sample was kept at 32°C in all experiments.

2.6. Energy transfer determination

The energy transfer efficiency between the Trp of HSA as donor and the bound porphyrin as acceptor was calculated on the basis of the Förster type resonance energy transfer theory.

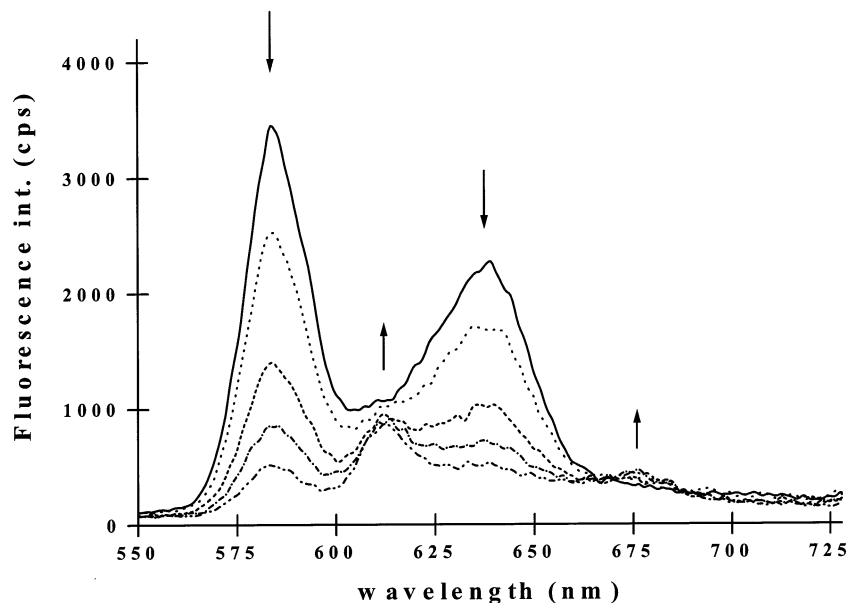


Fig. 1. Changes in the fluorescence emission spectrum of aqueous MgMP (50 nM, at pH 7.4) during a 3 h time period excited at 403 nm. The arrows show the characteristic change of the spectrum at the given wavelength as a function of time.

(Förster, 1959; Loura et al., 1996). Fluorescence lifetime measurements were used to determine k_{ET} the energy transfer rate as defined by the formula (Birks, 1970):

$$k_{ET} = \frac{1}{\tau_p} - \frac{1}{\tau} \quad (2)$$

where τ_p and τ were the fluorescence lifetimes of Trp/HSA in the presence and absence of porphyrin, respectively. According to the theory, k_{ET} is related to R , the distance between the donor and acceptor, by the following formula:

$$k_{ET} = \frac{8.8 \cdot 10^{-5} \cdot \kappa^2 \cdot Q_{Trp} \cdot J}{R^6 \cdot n^4 \cdot \tau} \quad (3)$$

where J is the spectral overlap between donor emission and acceptor absorption; Q_{Trp} is the quantum yield of Trp emission, n is the refractive index in the protein, and κ^2 is a factor depending on the relative orientation of the transition dipoles of the donor and the acceptor (Birks, 1970; Lakowitz, 1983b; Hochstrasser and Negus, 1984).

3. Results

3.1. Steady-state studies

3.1.1. Stability of porphyrin derivatives

The photostability of the chromophores is a requirement for the correct determination of the association constant based on the fluorescence intensity. The stability of MP and MgMP was controlled in the systems that we studied by measuring the fluorescence intensity of the porphyrin derivatives upon prolonged irradiation. The samples containing MP were found stable; but in case of MgMP the demetallation of the Mg-porphyrin in aqueous solution could be detected (Darwent et al., 1982). In Fig. 1 the typical changes of the emission spectrum as a function of time for MgMP in pH 7.4 phosphate buffer solution can be seen within 3 h. The emission maximum at 583.5 nm decreases and a new peak, with increasing intensity, characteristic for MP at 613 nm is observed. The effect was less significant when MgMP was incorporated in the liposomes or in

HSA. The rate constants of MgMP decomposition in the studied systems are listed in Table 1. The values in the Table represent the average of three independent measurements at 32°C. The data demonstrate the stabilising effect of liposomes and HSA for the MgMP, compared to that of the pure aqueous phase.

3.1.2. General spectral properties

The fluorescence emission spectra of MP and MgMP in buffer and in different complexed forms are shown in Fig. 2. The wavelength of excitation and emission maxima of the two dyes in different systems are listed in Table 2. The spectral characteristics in the buffer solution are in accordance with the literature data found for MgMP (Gouterman, 1961) and for MP (Margalit and Rotenberg, 1984). The addition of HSA and liposome to the MP solution resulted in an increase of fluorescence intensity (not seen in Fig. 2 because of normalisation) and in a significant red-shift of original fluorescence maximum of porphyrin. In case of MgMP the interaction with HSA and liposomes was followed by the increase of the fluorescence intensity, the spectral shifts were not significant.

The relative position of the emission maxima for protein-bound and liposome-bound molecules (see Fig. 2) are distinct in case of the two porphyrins. The effect is especially remarkable for MP, suggesting that the binding means different structural effects in the two cases.

Table 1

The rate constant of MgMP decomposition in different solvents at 32°C

Solvent	Rate constant (s ⁻¹)
Ethanol	2.5×10^{-5}
pH 7.4 Phosphate buffer	3.0×10^{-4}
HSA in pH 7.4 phosphate buffer	1.7×10^{-4}
Liposomes in pH 7.4 phosphate buffer	4.0×10^{-5}
Liposomes+HSA in pH 7.4 phosphate buffer	1.0×10^{-4}

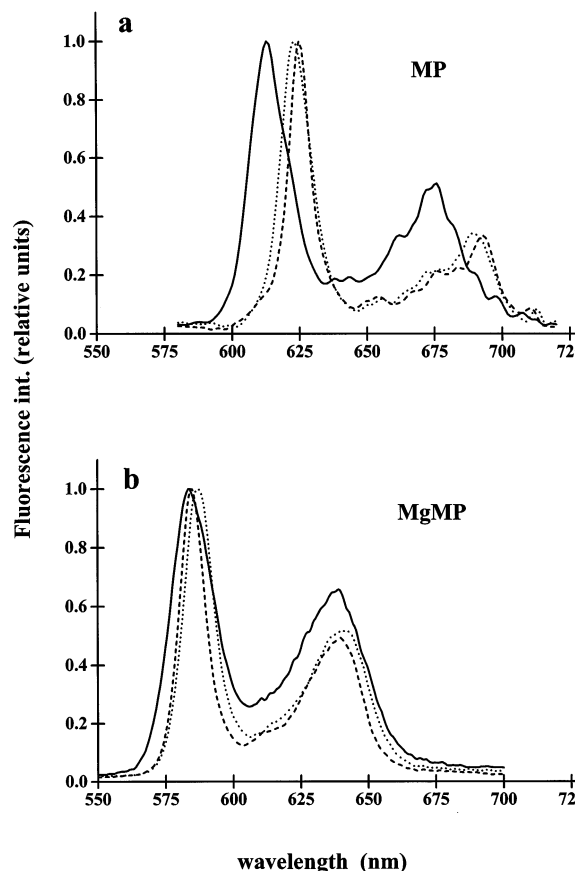


Fig. 2. (a) The normalised fluorescence emission spectra of MP in different systems at 32°C. The concentration of MP was 50 nM, in 10 mM pH 7.4 phosphate buffer in all cases. The different systems are indicated by different styles of lines. Solid line: MP in buffer; dashed line: MP in DMPC/DMPG liposome solution, at 10^{-4} M lipid concentration; dotted line: MP in $5 \cdot 10^{-6}$ M HSA solution. (b) The normalised fluorescence emission spectra of MgMP in different systems at 32°C. The concentration of MgMP was 50 nM, in 10 mM pH 7.4 phosphate buffer in all cases. The different systems are indicated by different styles of lines. Solid line: MgMP in buffer; dashed line: MgMP in DMPC/DMPG liposome solution, at 10^{-4} M lipid concentration; dotted line: MgMP in $5 \cdot 10^{-6}$ M HSA solution.

3.1.3. Complex formation of the porphyrins with HSA

In order to study the binding of MP and MgMP only to the high-affinity binding site of HSA, the amount of protein was added in excess in all measurements (Muller-Eberhard and Morf, 1975; Parr and Pasternack, 1977; Cannon et

Table 2

The wavelength of MP and MgMP fluorescence excitation and emission spectra maxima in different media at 32°C

Solvent	λ_{ex} (nm)		λ_{em} (nm)	
	MP	MgMP	MP	MgMP
DMF	399	—	624	—
Ethanol	—	406	—	583
pH 7.4 Phosphate buffer	392	403	613	584
HSA in pH 7.4 phosphate buffer	399	412	623	587
Liposome in pH 7.4 phosphate buffer	400	411	625	585

al., 1984; Rotenberg and Margalit, 1985; He and Carter, 1992). The plots of the relative fluorescence intensities of MP (at 623 nm) and of MgMP (at 587 nm), versus the total concentration of the added HSA are shown in the inset of the Fig. 3, and demonstrate a definite saturation effect. The association constant K_a , for the porphyrin—HSA reaction was determined from a Scatchard representation (Scatchard, 1949), as shown in Fig. 3. This method can also be used to determine the number of binding sites, n and to differentiate between the co-operative and non co-operative binding of ligands (Schwarz, 1976). In our experiments the Scatchard plots correspond to the following formula:

$$K_a \cdot (n[P]_{\text{tot}} - [\text{HSA}]_{\text{bound}}) = \frac{[\text{HSA}]_{\text{bound}}}{[\text{HSA}]_{\text{free}}} \quad (4)$$

where $[\text{HSA}]_{\text{bound}}$ represents the concentration of HSA that binds porphyrins; and $[\text{HSA}]_{\text{free}}$ is the concentration of the protein, without bound porphyrin. When plotting the values of $([\text{HSA}]_{\text{bound}}/[P]_{\text{tot}})/[\text{HSA}]_{\text{free}}$ against $[\text{HSA}]_{\text{bound}}/[P]_{\text{tot}}$, the graph should indicate linear relationship. The intercepts of the fitted straight line at the x and y axes yield n and $n \cdot K_a$, respectively.

At the applied experimental conditions, the direct determination of $[\text{HSA}]_{\text{bound}}$ was impossible, so we had to approximate it. Because of the relatively large excess of HSA at all experiments we supposed that only the main binding site of HSA takes part in the complex formation thus $[\text{HSA}]_{\text{bound}}$ was estimated by the bound porphyrin concentration, $[P]_{\text{bound}}$. The concentration of free porphyrin, $[P]_{\text{free}}$ was determined from the initial porphyrin concentration $[P]_{\text{tot}}$, and from the

fluorescence intensities at that wavelength where there is negligible overlap in the emission spectrum of pure and HSA containing porphyrin solutions (for MP at 605 nm, and for MgMP at 570 nm, respectively). The data points could be well fitted by a straight line for both systems. The average of n values for MP (0.92 ± 0.03), and for MgMP (1.01 ± 0.04) calculated from the intersections indicate the validity of the Scatchard description with $n=1$, which means a non co-operative binding of these porphyrins to one single type of binding sites of HSA at the applied conditions. The association constants for the MP- and MgMP-HSA complex formations are given in Table 3. The error of the MgMP-HSA association constant caused by the instability of MgMP was calculated on the basis of the measured rate constants of demetallation reaction. According to these data (Table 1) the error was estimated as being less than 6% under the applied experimental conditions, what we considered as an inherent inaccuracy in the experiments.

3.1.4. Interaction of MP and MgMP with liposomes

The experimental conditions to characterise the interactions between the DMPC/DMPG SUV liposomes and the porphyrin derivatives were similar to those, described above. The aliquots of liposomes (to vary the total lipid concentration of the solution from $5 \cdot 10^{-6}$ to $2 \cdot 10^{-4}$ M) were added stepwise under stirring, and the fluorescence emission spectra were recorded.

To determine the association constant K_L of porphyrins to the liposome, the following formula (Kuzelova and Brault, 1994) was used:

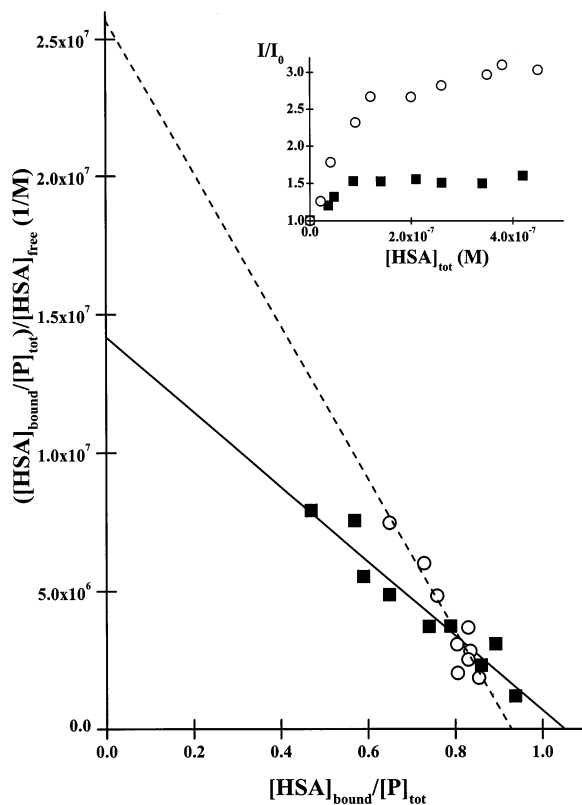


Fig. 3. The Scatchard representation and fitted straight lines for MP-HSA (open circles and dashed line), and MgMP-HSA (solid squares and solid line) systems, at pH 7.4 and at 32°C, to determine the porphyrin-HSA association constants. The inset shows the relative fluorescence intensities versus the total concentration of added HSA for both cases (the symbols are the same as mentioned above). The excitation and emission wavelengths for MP-HSA were 392 and 623 and for MgMP-HSA solution 403 and 587 nm, respectively. The porphyrin concentration was 50 nM.

$$\frac{1}{I - I_0} = \frac{1}{(I_{\text{lip}} - I_0) \cdot K_L [\text{lip}]} + \frac{1}{I_{\text{lip}} - I_0} \quad (5)$$

where [lip] represents the lipid concentration corresponding to the free liposomes in the solution,

Table 3

The association constants of MP and MgMP to HSA (K_a) and liposomes (K_L) at 32°C

Porphyrin	$K_a \text{ (M}^{-1}\text{)}$	$K_L \text{ (M}^{-1}\text{)}$
MP	$(2.5 \pm 0.7) \times 10^7$	$(3.2 \pm 0.6) \times 10^4$
MgMP	$(1.7 \pm 0.5) \times 10^7$	$(1.5 \pm 0.6) \times 10^4$

and the fluorescence intensities are determined at the wavelength of peak emission of porphyrin bound to liposomes; I_0 , I and I_{lip} are the emission intensities in the absence, in the presence of liposomes and in the case of total incorporation respectively. This formula takes into account the possible overlap of emission bands of free and bound porphyrins. To evaluate the association constant of the examined porphyrins to the DMPC/DMPG SUV liposomes, we used the intensities at the emission peak: for MP bound to liposome at 625 nm, and for the MgMP-liposome system at 585 nm.

Because of the large concentration difference (three orders of magnitude or bigger) between the porphyrin and lipid in our experiments, the lipid concentration in the equilibrium was approximated by the total lipid concentration. Accordingly, the plot of $I_0/(I - I_0)$ as a function of $1/[\text{lip}]_{\text{tot}}$ should yield a straight line with an intercept at the y axis as $I_0/(I_{\text{lip}} - I_0)$, and with a slope as $I_0/[(I_{\text{lip}} - I_0) \cdot K_L]$. The binding constants for the porphyrin-liposome interaction were evaluated from the parameters of the fitted function. Fig. 4 represents a typical plot of the MP- and MgMP-lipid systems. The K_L values are listed in Table 3. The inaccuracy of the association constant caused by the demetallation process in case of the MgMP-liposome system is similar to that found for the MgMP-HSA complex.

3.1.5. The distribution of porphyrins between HSA and the liposomes

In the partition experiments liposomes corresponding to the saturation value were added to MP and MgMP dissolved in buffer. To complete the incorporation reaction, the sample was incubated for 5 min then increasing amounts of HSA were added to it. The emission spectrum of MP and MgMP was recorded at different HSA-liposome molar ratios, excited at the Soret maximum. The fluorescence intensity of the porphyrin-liposome complex decreased with the increase of HSA concentration, and a virtual shift of the spectrum indicated the appearance of a new compound. The spectral change corresponded to the appearance of the MP and MgMP spectra when bound to HSA.

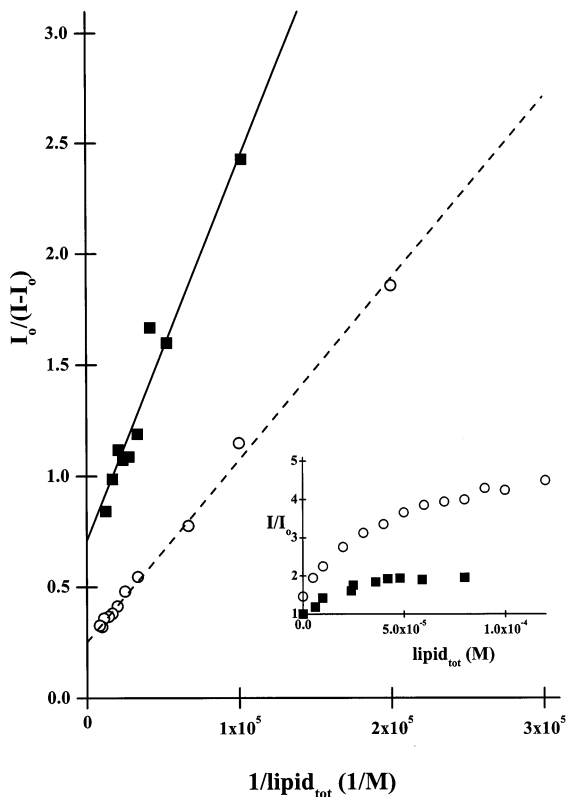


Fig. 4. The relative fluorescence intensity change as the function of total liposome concentration in the MP-liposome (open circles and dashed line) and MgMP-liposome (solid squares and solid line) solutions, at pH 7.4, to determine the K_L values. The lines indicate the fitted functions. The inset represent the relative emitted fluorescence light intensities plotted against the lipid concentration. The excitation and emission wavelengths for MP-liposome were 392 and 625 and for MgMP-liposome solution 403 and 585 nm, respectively. The porphyrin concentration in all cases was constant, 50 nM, and the temperature was kept at 32°C.

If the partition is the result of the competition of two independent complex forming reactions through the aqueous phase, the experimental data obey the following formula (Kuzelova and Brault, 1994):

$$\frac{K_L \cdot [\text{lip}]}{K_L \cdot [\text{lip}] + K_a[\text{HSA}]} = \frac{I - I_{\text{HSA}}}{I_{\text{lip}} - I_{\text{HSA}}} \quad (6)$$

where I_{lip} and I_{HSA} are the fluorescence intensities of the porphyrin at the wavelength of porphyrin–liposome emission maximum, when bound to

liposome or to HSA, respectively and I is the actual measured intensity at the same wavelength.

In Fig. 5 one series of measurements for both porphyrin derivatives are shown. The data suggests that both porphyrins rebind to HSA, but the process is different for the free-base and for the metallo-porphyrin. The increase of HSA concentration in the MgMP-liposome system resulted in a monotonous decrease of the fluorescence intensity at 585 nm that demonstrates the total transfer of Mg-porphyrin from the liposomes to the HSA molecules. The saturation value of this intensity decrease is determined by the fluorescence intensity

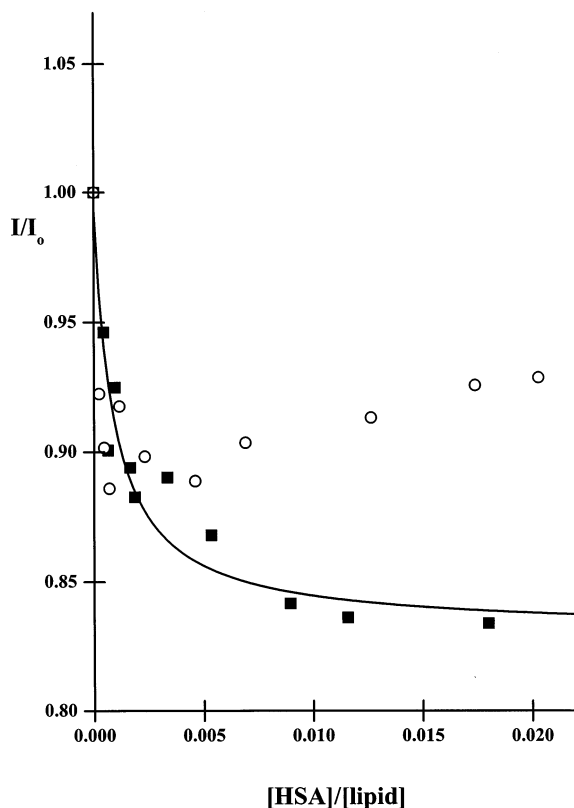


Fig. 5. The distribution of MP (open circles) and MgMP (solid squares) between liposomes and HSA. The relative fluorescence intensities at wavelengths of the emission maximum for porphyrin–liposome complexes plotted against the HSA/lipid ratio, at pH 7.4. (The emission maximum for MP was 625 nm and for MgMP 585 nm, respectively.) The porphyrin concentration for both derivatives was 50 nM, and the temperature was 32°C. The solid curve demonstrate the fitted function to the data points of MgMP containing HSA-liposome system.

Table 4
The fluorescence lifetime of MP and MgMP in different solvents at 32°C

Solvent	Lifetime (ns)	
	MP	MgMP
DMF	17.95 ± 0.12	8.86 ± 0.12
Ethanol	14.45 ± 0.12	7.45 ± 0.09
pH 7.4 Phosphate buffer	15.10 ± 0.11	8.05 ± 0.25
HSA in pH 7.4 phosphate buffer	16.53 ± 0.16	9.55 ± 0.22
Liposome in pH 7.4 phosphate buffer	18.10 ± 0.11	10.62 ± 0.27

sity of MgMP when it becomes totally bound to HSA. In Fig. 5, the solid line shows a fitted function according to Eq. (6) for the MgMP partition data. The fitting resulted in K_a : $1.9 \cdot 10^7 \text{ M}^{-1}$ and K_L : $1.7 \cdot 10^4 \text{ M}^{-1}$ for MgMP binding, that agree well with those obtained by the independent experiments for binding to HSA and to liposomes, respectively.

The relative fluorescence intensity of the MP-lipid solution at 625 nm shows a similar change at low protein concentrations, while a well defined increase of this parameter can be seen above 0.005 [HSA]/[lip] concentration ratio, up to a saturation value.

3.2. Time-resolved measurements

3.2.1. The fluorescence lifetime of porphyrin derivatives

The excited state lifetime data were also used to compare the complex formation of the two porphyrin derivatives with HSA or liposomes. The instability of MgMP, however, caused serious problems in the measurements, since the low concentration of the sample required long data collection time. Thus the values for MgMP are valid within an accuracy of $\pm 30\%$. From the data, compared in Table 4, it is seen that the deexcitation pathways in the various environments are not significantly different in case of the two porphyrins.

3.2.2. The fluorescence lifetime of the tryptophan in HSA

The fluorescence lifetime of the single tryptophan in HSA—near the porphyrin main binding site (Meloun et al., 1975; He and Carter, 1992)—might be a sensitive parameter to detect the binding of porphyrins to HSA from the side of the protein, as the spectral overlap between the porphyrins and the Trp allows for energy transfer.

To make the emitted signal large enough for the accurate time resolved measurements, the initial concentration of HSA in these experiments was $6 \cdot 10^{-6} \text{ M}$, and the porphyrin/protein ratio was kept below 1, to saturate only the main binding site of HSA. The Trp fluorescence was excited at 295 nm, and the emission was detected at the maximum, at 345 nm. This maximum position corresponds to a moderately solvent exposed Trp environment in HSA (Lakowitz, 1983b).

The fluorescence of Trp was quenched by both porphyrins with a saturation character. The long lifetime components of a two component fit to the fluorescence decay of Trp at saturation conditions are shown in Table 5, together with the corresponding k_{ET} (Eq. (3)) values.

The J overlap integrals needed for the calculations were determined by the following formula:

$$J = \int_{300}^{500} F_{\text{Trp}}(\lambda) \cdot \epsilon_0(\lambda) \cdot \lambda^4 \cdot d\lambda \quad (7)$$

where $F_{\text{Trp}}(\lambda)$ is the normalised fluorescence spectrum of Trp, $\epsilon_0(\lambda)$ is the molar extinction coefficient of MP or MgMP (in $\text{M}^{-1}\text{cm}^{-1}$) and λ is measured in nm (Loura et al., 1996). The other parameters in Eq. (3) were estimated by using $n = 1.35$, $Q_{\text{Trp}} = 0.35$ according to Longworth (Longworth, 1971). The obtained J values, shown also in Table 5, are comparable with literature data for similar systems. The distances between the Trp in HSA and the bound porphyrins were compared (Table 5) by using Eq. (3), assuming that the orientation factor, κ^2 is equal to 2/3 in both cases. This κ^2 value corresponds to a freely rotating system, which is acceptable for the Trp at the applied conditions (Birks, 1970).

Table 5

The influences of the energy transfer between the Trp of HSA and porphyrin derivatives at 32°C

System	τ (ns)	k_{ET} (s^{-1})	J ($\text{M}^{-1} \cdot \text{cm}^3$)	R (nm)
HSA	5.76 ± 0.11	—	—	—
HSA + MP	4.80 ± 0.11	3.47×10^{-11}	7.53×10^{-14}	5.3
HSA + MgMP	4.27 ± 0.14	6.06×10^{-11}	4.19×10^{-14}	4.4

4. Discussion

4.1. Interaction of MP and MgMP with HSA

The spectral shifts of emission spectra and the changes in the fluorescence lifetime of the porphyrins, and Trp residue in HSA support the interaction of MP and MgMP with HSA at our experimental conditions. The calculated R values (Table 5) are comparable with the size of the HSA molecule and with a possible distance between the porphyrins bound to the primary binding site in HSA and the nearby Trp according to the low resolution X-ray crystallographic results for the structure of HSA (He and Carter, 1992).

We compared the K_a values, evaluated from the results of steady state measurements for MP ($2.5 \cdot 10^7$) and MgMP ($1.7 \cdot 10^7$) porphyrin derivatives with literature data for similar systems ($5 \cdot 10^5 - 3 \cdot 10^8 \text{ M}^{-1}$) (Muller-Eberhard and Morgan 1975, Reddi et al., 1981; Rotenberg et al., 1987) and a good agreement could be observed. It was found that the association constant of different free-base porphyrins increases with the hydrophobicity of the side chains of the porphyrins. The values reported for hematoporphyrin and for deuteroporphyrin are $\sim 10^6$ and $\sim 5 \cdot 10^7 \text{ M}^{-1}$, respectively. The association constant, determined by us for MP, is between these values, in accordance with the hydrophobic character of this molecule compared to the other porphyrin derivatives.

The association constants in Table 3 suggest tighter contact in case of MP-HSA (the K_a value for this system is almost 2-fold larger) compared to the MgMP-HSA interaction. We explain the difference in the K_a values on the basis of distinct configurations: the porphyrin ring is expected to be planar in case of MP (Scheidt, 1978), but the

presence of the Mg ion—in most solvents/environments—modifies this planarity into square pyramidal geometry, where the distance of the ion from the ring may vary with co-ordination (Buckler, 1978). The X-ray structure analysis of different Mg-porphyrins (Tronrud et al., 1986) demonstrated, that the distance of the Mg^{2+} from the main porphyrin plane (0.42–0.54 Å) can vary depending mainly on the nature of the ligand and on the side chains, attached to the main core. The protein environment thus may also have a similar effect.

4.2. Binding of MP and MgMP to liposomes

The interaction of the porphyrin derivative with the different membrane structures of the living systems are critical in the transport and final distribution of these molecules. The porphyrin binding and incorporation by several types of liposomes and cell membranes was studied by using different methods (Greenbaum and Kappas, 1994b; Kuzelova and Brault, 1994; Ricchelli et al., 1995). The surface charge of the liposomes, the charge distribution of the porphyrin derivative and the hydrophobic interactions are the most important factors in the binding and incorporation effects, at a given pH and ionic strength.

We compared the K_L value of MP obtained by us ($K_L = 3.2 \cdot 10^4$) to that found for deuteroporphyrin with respect to DMPC sonicated liposomes as $\sim 8 \cdot 10^4 \text{ M}^{-1}$ (Kuzelova and Brault, 1994, 1995). The slight difference between the two values may be explained by the different surface charge distribution of liposomes and by the difference in the hydrophobic nature of the two porphyrins. In the cited works, it was suggested that the porphyrin is located between the polar and apolar part of the DMPC liposomes. In our

studies, the fluorescence emission maximum of MP in the liposome (Fig. 2) is close to that observed in DMF (Table 2). This suggests that the environment of the porphyrin has similar hydrophobicity in the two systems. This means that the slightly negative surface of the liposome might assist the effective incorporation of MP into the deeper apolar part of the liposomes in our case.

The results obtained for the uptake of Zn-mesoporphyrin by differently charged liposomes (Greenbaum and Kappas, 1994b) showed that this porphyrin is incorporated closer to the polar region of the bilayer. The same charge and the similar size of Zn and Mg ions may result in similar non polar geometry and charge distribution for both metallo-porphyrins leading to the assumption that the co-ordination of MgMP is similar to that of ZnMP in liposomes. This conclusion is also supported by the fact that there is only a slight spectral shift when MgMP is bound to liposomes compared to the aqueous or ethanol solutions

4.3. Partition of MP and MgMP between liposomes and HSA

In our studies we examined the partition of free-base and MgMP between the DMPC/DMPG liposomes and HSA based on the hypothesis of Brault et al. (Kuzelova and Brault, 1994).

The results obtained by us (Fig. 5) indicated that the same model describes the redistribution of MgMP. But the partition of MP between the liposomes and the HSA showed a different character. The agreement between the experimentally measured points and the fitted function was sufficient only for the initial part of the redistribution process. The rebinding of the free-base MP from the liposome to HSA seemed to be hindered when the amount of HSA exceeded a certain [HSA]/[liposome] ratio. This suggests that the partition of MP between the liposome and HSA are not independent processes.

In the literature there is evidence for the binding of serum albumin to liposomes of various compositions (Lis et al., 1976; Hoekstra and Scherphof, 1979). This interaction might result in

the penetration of the protein molecules into the lipid phase. Furthermore, it was suggested that the non-incorporated moiety of the protein may cover the surface of the liposomes (Law et al., 1988; Galántai et al., 1996). A covering effect in case of the MP incorporated liposomes that becomes dominant with increasing HSA concentration would explain our results as well. We interpret the results of the partition experiment for the MP in this way, and suppose that the interaction of HSA with the liposomes prevents the efflux of porphyrin to the aqueous phase. The increase in the fluorescence intensity of MP towards higher HSA concentrations (Fig. 5) can be explained as an effect of the modification of the MP environment due to the HSA–liposome interactions.

The striking difference in the redistribution of the two porphyrins indicates that the interaction of liposomes with HSA is affected by the incorporation of the porphyrin derivatives. The presence of MgMP on the surface of the liposomes, or near to it prevents the tighter co-ordination of HSA to the lipid membrane; the redistribution of porphyrin—governed by the difference in the association constants—occurs through the aqueous phase. In case of the MP-liposome system, where the porphyrin is incorporated into the deeper part of the liposome, the HSA–liposome interaction generate new conditions for the partition of porphyrin between the two phases.

The distinct partition behaviour of the two porphyrins between lipid membranes of certain composition and HSA, in addition to the slight differences in the porphyrin–HSA and porphyrin–liposome association constants, may result in a notable difference in the metabolic transport of free-base and metallo-porphyrin analogues. These effects should be considered also with respect to the selection of proper method for photodynamic tumor therapy.

References

- Birks, J.B., 1970. *Photophysics of Aromatic Molecules*. Wiley Interscience, London, pp. 87–90.

- Bonett, R., White, R.D., Winfield, U.J., Berenbaum, M.C., 1989. Hydroporphyrins of the *meso*-tetra(hydroxyphenyl) porphyrin series as tumour photosensitizers. *Biochem. J.* 261, 277–280.
- Brault, D., 1990. Physical chemistry of porphyrins and their interactions with membranes: the importance of pH. *J. Photochem. Photobiol. B: Biol.* 6, 79–86.
- Buckler, J.W., 1978. Synthesis and properties of metalloporphyrins. In: Dolphin, D. (ed.), *The Porphyrins*, vol. 1. Academic Press New York, pp. 425–427.
- Cannon, J.B., Kuo, F.S., Pasternack, F., Wong, N.M., Muller-Eberhard, U., 1984. Kinetics of the interaction of heme liposomes with heme binding proteins. *Biochemistry* 23, 3715–3721.
- Darwent, J.R., Douglas, P., Harriman, A., Porter, G., Richoux, M.-C., 1982. Metal phthalocyanines and porphyrins as photosensitizers for reduction of water to hydrogen. *Coord. Chem. Rev.* 44, 83–126.
- Förster, T., 1959. Transfer mechanism of electronic excitation. *Disc. Faraday Soc.* 27, 7–17.
- Fukuda, H., Paredes, S., Battle, A.M. del C., 1992. Tumour-localizing properties of porphyrins. In vivo studies using free and liposome encapsulated aminolevulinic acid. *Comp. Biochem. Physiol.* 102B, 433–436.
- Galántai, R., Balog, E., Tölgyesi, F., Fidy, J., 1996. The role of serum albumin in porphyrin metabolism. A fluorescence study. *Biophys. J.* 70, A154.
- Geze, M., Morliere, P., Maziere, J.C., Smith, K.M., Santus, R., 1993. Lysosomes, a key target of hydrophobic photosensitizers proposed for photochemotherapeutic applications. *J. Photochem. Photobiol. B: Biol.* 20, 23–35.
- Gouterman, M., 1961. Spectra of porphyrins, *J. Mol. Spectrosc.* 6, 138–163.
- Greenbaum, N.L., Kappas, A., 1994a. Distribution of metalloporphyrin inhibitors of heme oxygenase among serum transport proteins. *Pharmacology* 49, 205–214.
- Greenbaum, N.L., Kappas, A., 1994b. Incorporation of metalloporphyrin inhibitors of heme oxygenase into micelles and liposomes. *Pharmacology* 49, 215–225.
- He, X.M., Carter, D.C., 1992. Atomic structure and chemistry of human serum albumin. *Nature* 358, 209–215.
- Henderson, B.W., Dougherty, T.J., 1992. How does photodynamic therapy work? *Photochem. Photobiol.* 55, 145–157.
- Hochstrasser, R.M., Negus, D.K., 1984. Picosecond fluorescence decay of tryptophans in Myoglobin. *Proc. Natl. Acad. Sci. USA* 81, 4399–4403.
- Hoekstra, D., Scherphof, G., 1979. Effect of fetal calf serum and serum protein fractions on the uptake of liposomal phosphatidylcholine by rat hepatocytes in primary monolayer culture. *Biochem. Biophys. Acta* 551, 109–121.
- Kagawa, Y., 1974. Components of the mitochondrial membrane. In: Korn, E.D. (ed.), *Methodes in Membrane Biology*, vol. 1. Plenum Press, New York, pp. 201–235.
- Kennedy, J.C., Pottier, R.H., 1992. Endogenous protoporphyrin IX, a clinically useful photosensitizer for photodynamic therapy. *J. Photochem. Photobiol. B: Biol.* 14, 275–292.
- Kessel, D., Dougherty, T.J., Chang, C.K., 1991. Photosensitization by synthetic diporphyrins and dichlorins in vivo and in vitro. *Photochem. Photobiol.* 53, 475–479.
- Kuzelova, K., Brault, D., 1994. Kinetic and equilibrium studies of porphyrin interactions with unilamellar lipidic vesicles. *Biochemistry* 33, 9447–9459.
- Kuzelova, K., Brault, D., 1995. Interaction of dicarboxylate porphyrins with unilamellar lipidic vesicles: drastic effect of pH and cholesterol on kinetics. *Biochemistry* 34, 11245–11255.
- Lakowitz, J.R., 1983a. Principles of Fluorescence Spectroscopy, vol. 44. Plenum Press, New York, pp. 303–316.
- Lakowitz, J.R., 1983b. Principles of Fluorescence Spectroscopy. Plenum Press, New York, pp. 187–189.
- Law, S.L., Lo, W.Y., Pai, S.H., Teh, G.W., 1988. The electrokinetic behaviour of liposomes adsorbed with bovine serum albumin. *Int. J. Pharm.* 43, 257–260.
- Lis, L.J., Kauffman, J.W., Shriver, D.F., 1976. Raman spectroscopic detection and examination of the interaction of amino acids, polypeptides and proteins with the phosphatidylcholine lamellar structure. *Biochim. Biophys. Acta* 436, 513–522.
- Loh, C.S., Vernon, D., MacRobert, A.J., Bedwell, J., Brown, S.G., Brown, S.B., 1993. Endogenous porphyrin distribution induced by 5-aminolaevulinic acid in the tissue layers of the gastrointestinal tract. *J. Photochem. Photobiol. B: Biol.* 20, 47–54.
- Longworth, J.W., 1971. Excited States of Proteins and Nucleic Acids, Steiner, R.F., Weinryb, I. (eds.). Plenum Press, New York, pp. 319–484.
- Loura, L.M.S., Fedorov, A., Prieto, M., 1996. Resonance energy transfer in a model system of membranes: application to gel and liquid crystalline phases. *Biophys. J.* 71, 1823–1836.
- Margalit, R., Rotenberg, M., 1984. Thermodynamics of porphyrin dimerization in aqueous solutions. *Biochem. J.* 219, 445–450.
- Meloun, B., Moravek, L., Kostka, V., 1975. Complete amino acid sequence of human serum albumin. *FEBS Lett.* 58, 134–137.
- Moan, J., Berg, K., 1992. Photochemotherapy of cancer: experimental research. *Photochem. Photobiol.* 55, 931–948.
- Moan, J., Christensen, T., 1981. Cellular uptake and photodynamic effect of hematoporphyrin. *Photobiochem. Photobiophys.* 2, 291–299.
- Muller-Eberhard, U., Morgan, W.T., 1975. Porphyrin binding proteins in serum. *Ann. New York Acad. Sci.* 244, 624–650.
- Parr, G.P., Pasternack, R.F., 1977. The interaction of some water-soluble porphyrins and metalloporphyrins with human serum albumin. *Bioinorg. Chem.* 7, 277–282.
- Reddi, E., Ricchelli, F., Jori, G., 1981. Interaction of human serum albumin with hematoporphyrin and its Zn^{2+} and Fe^{3+} derivatives. *Int. J. Peptide Protein Res.* 18, 402–408.
- Ricchelli, F., 1995. Photophysical properties of porphyrins in biological membranes. *J. Photochem. Photobiol. B: Biol.* 29, 109–118.

- Ricchelli, F., Gobbo, S., Jori, G., Salet, C., Moreno, G., 1995. Temperature-induced changes in fluorescence properties as probe of porphyrin microenvironment in lipid membranes 2. The partition of hematoporphyrin and protoporphyrin in mitochondria. *Eur. J. Biochem.* 233, 165–170.
- Ricchelli, F., Jori, G., Moreno, G., Vinzens, F., Salet, C., 1990. Factors influencing the distribution pattern of porphyrins in cell membranes. *J. Photochem. Photobiol. B: Biol.* 6, 69–77.
- Rosenbach-Belkin, V., Chen, L., Fiedor, L., Tregub, I., Pavlotsky, F., Brumfeld, V., Salomon, Y., Scherz, A., 1996. Serine conjugates of chlorophyll and bacteriochlorophyll: photocytotoxicity in vitro and tissue distribution in mice bearing melanoma tumors. *Photochem. and Photobiol.* 64, 174–181.
- Rosenberger, V., Margalit, R., 1993. Thermodynamics of the binding of hematoporphyrin ester, a hematoporphyrin derivative-like photosensitizer, and its components to human serum albumin, human high-density lipoprotein and human low-density lipoprotein. *Photochem. Photobiol.* 58, 627–630.
- Rotenberg, M., Margalit, R., 1985. Deuteroporphyrin-albumin binding equilibrium, *Biochem. J.* 229, 197–203.
- Rotenberg, M., Cohen, S., Margalit, R., 1987. Thermodynamics of porphyrin binding to serum albumin: effects of temperature, of the porphyrin species and of albumin-carried fatty acids. *Photochem. Photobiol.* 46, 689–693.
- Rouser, G., 1969. Two dimensional thin layer chromatographic separation of polar lipids and determination of phospholipids by phosphorus analysis of spots. *Lipids* 5, 494–496.
- Scatchard, G., 1949. The attractions of proteins for small molecules and ions. *Ann. New York Acad. Sci.* 51, 660–672.
- Scheidt, W.R., 1978. Porphyrin stereochemistry. In: Dolphin, D. (ed.), *The Porphyrins*, vol. 3. Academic Press, New York, pp. 482–501.
- Schwarz, G., 1976. Some general aspects regarding the interpretation of binding data by means of a scatchard plot. *Biophys. Struct. Mechanism* 2, 1–12.
- Senge, M.O., 1992. The conformational flexibility of tetrapyrroles—current model studies and photobiological relevance. *J. Photochem. Photobiol. B: Biol.* 16, 3–36.
- Spikes, J.D., 1986. Phtalocyanins as photosensitizers in biological systems and for the photodynamic therapy of tumors. *Photochem. Photobiol.* 43, 691–699.
- Tronrud, D.E., Schmid, M.F., Matthews, B.W., 1986. Structure and X-ray amino acid sequence of a bacteriochlorophyll a protein from *Prosthecochloris aestuarii* refined at 1.8 Å resolution. *J. Mol. Biol.* 188, 443–454.
- Vever-Bizet, C., Brault, D., 1993. Kinetics of incorporation of porphyrins into small unilamellar vesicles. *Biochim. Biophys. Acta* 1153, 170–174.